

# Thermopower enhancement from engineering the $\text{Na}_{0.7}\text{CoO}_2$ interacting fermiology via Fe doping

Raphael Richter,<sup>1</sup> Denitsa Shopova,<sup>2</sup> Wenjie Xie,<sup>2</sup> Anke Weidenkaff,<sup>2</sup> and Frank Lechermann<sup>1,3</sup>

<sup>1</sup>*Institut für Theoretische Physik, Universität Hamburg, 20355 Hamburg, Germany*

<sup>2</sup>*Chemische Materialsynthese, Institut für Materialwissenschaft, Universität Stuttgart, 70569 Stuttgart, Germany*

<sup>3</sup>*Institut für Keramische Hochleistungswerkstoffe, Technische Universität Hamburg-Harburg, 21073 Hamburg, Germany*

The sodium cobaltate system  $\text{Na}_x\text{CoO}_2$  is a prominent representant of strongly correlated materials with promising thermoelectric response. In a combined theoretical and experimental study we show that by doping the Co site of the compound at  $x=0.7$  with iron, a further increase of the Seebeck coefficient is achieved. The Fe defects give rise to effective hole doping in the high-thermopower region of larger sodium content  $x$ . Originally filled hole pockets in the angular-resolved spectral function of the material shift to low energy when introducing Fe, leading to a multi-sheet interacting Fermi surface. Because of the higher sensitivity of correlated materials to doping, introducing adequate substitutional defects is thus a promising route to manipulate their thermopower.

*Introduction.* Selected compounds subject to strong electronic correlations display a remarkable thermoelectric response. Layered cobaltates composed of stacked triangular  $\text{CoO}_2$  sheets are of particular interest because of their large doping range. High thermopower above  $75\mu\text{V}/\text{K}$  has originally been detected in the  $\text{Na}_x\text{CoO}_2$  system at larger sodium doping  $x \sim 0.7$  [1–4]. Even higher Seebeck coefficients and increased figure of merit have been measured for misfit cobaltates (see e.g. [5] for a recent review). Due to the simpler crystal structure, the small-unit-cell sodium-compound system remains of key interest in view of the essential electronic-structure effects underlying the pronounced thermoelectric response.

The high-thermopower region is associated with clear signatures of strong electronic correlations. Charge disproportionation [6, 7], change of Pauli-like magnetic susceptibility to Curie-Weiss-like behavior [8] and eventual onset of in-plane ferromagnetic (FM) order [7, 9–15] at  $x=0.75$  are observed. Moreover the region displays unique low-energy excitations [16].

Several theoretical works addressed the thermoelectricity of  $\text{Na}_x\text{CoO}_2$  [17–23], ranging from applications of Heikes formula, Boltzmann-equation approaches as well as Kubo-formula-oriented modelings. Correlation effects described beyond conventional density functional theory (DFT) indeed increase the thermopower. Depending on  $x$ , the oxidation state of cobalt nominally reads  $\text{Co}^{(4-x)+}(3d^{5+x})$ . A strong cubic crystal field establishes a Co ( $t_{2g}, e_g$ ) low-spin state, and  $x$  controls the filling of the localized  $t_{2g}$  manifold. The additional trigonal crystal field splits  $t_{2g}$  into  $a_{1g}$  and  $e'_g$  levels. But the measured Fermi surface (FS) shows only a single distinct hole-like  $a_{1g}$ -dominated sheet centered around the  $\Gamma$  point [24, 25]. Hole pockets of mainly  $e'_g$  kind are suppressed by correlation effects [26, 27].

In this work we show that there is the possibility to engineer the interacting electronic structure of  $\text{Na}_x\text{CoO}_2$  in view of an extra increase of the thermoelectric response. Substitutional doping of the Co site with Fe is for  $x \sim 0.7$

effective in shifting the  $e'_g$  hole pockets to the Fermi level  $\varepsilon_F$ . The hole doping with iron also enforces the correlation strength. But different from the small- $x$  region where the thermopower is found to be rather weak, for  $\text{Na}_{0.7}\text{Co}_{1-y}\text{Fe}_y\text{O}_2$  the Seebeck coefficient is further enhanced. This finding paves the road for future design of thermoelectric transport in correlated materials.

*Theoretical approach.* An advanced charge self-consistent DFT + dynamical mean-field theory (DMFT) scheme [28] is utilized. The method is based on an efficient combination of the mixed-basis pseudopotential framework [29] with continuous-time quantum Monte-Carlo in the hybridization-expansion representation [30–33] for the DMFT impurity problem. The correlated subspace consists of projected [34, 35] Co/Fe  $3d(t_{2g})$  orbitals, i.e. a threefold many-body treatment holds in the single-site DMFT part. The generic multi-orbital Coulomb interaction is chosen in Slater-Kanamori parametrization with Hubbard  $U=5\text{eV}$  and Hund's exchange  $J_H=0.7\text{eV}$ . A double-counting correction of the fully-localized form [36] is used. We construct Na as well as Co pseudopotentials with fractional nuclear charge to cope with the doping scenario in a virtual-crystal approximation (VCA). Based on a primitive hexagonal cell for one formula unit  $\text{Na}_x\text{CoO}_2$ , the fractional-charged Na is in the so-called 'Na2' position, i.e. aside from the transition-metal position below. No bilayer splitting is included. The calculations are readily extendable to more complex unit cells and geometries, however the present approach suits the purpose of rendering general qualitative statements.

For the investigation of transport, the Kubo formalism based on the correlation functions

$$K_n = \sum_{\mathbf{k}} \int d\omega \beta^n (\omega - \mu)^n \left( -\frac{\partial f_\mu}{\partial \omega} \right) \times \text{Tr} [\mathbf{v}(\mathbf{k}) A(\mathbf{k}, \omega) \mathbf{v}(\mathbf{k}) A(\mathbf{k}, \omega)] , \quad (1)$$

is used in the DMFT context [22, 27, 37, 38]. Here

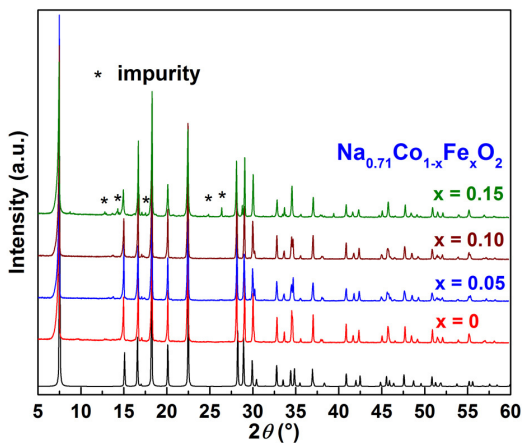


FIG. 1. (color online) XRD pattern of the  $\text{Na}_{0.71}\text{Co}_{1-y}\text{Fe}_y\text{O}_2$  ( $y = 0, 0.05, 0.10$  and  $0.15$ ) powder samples. Black line: reference data obtained from the ICSD database.

$\beta = 1/T$  is the inverse temperature,  $\mathbf{v}(\mathbf{k})$  denotes the Fermi velocity calculated from the charge self-consistent Bloch bands and  $f_\mu$  marks the Fermi-Dirac distribution. To extract the  $k$ -resolved one-particle spectral function  $A(\mathbf{k}, \omega) = -\pi^{-1} \text{Im} G(\mathbf{k}, \omega)$  from the Green's function  $G$ , an analytical continuation of the electronic self-energy in Matsubara space  $\omega_n$  is performed via the Padé approximation. For more details we refer to Ref. [27]. This framework allows us to compute the thermopower through  $S = -\frac{k_B}{|e|} \frac{K_1}{K_0}$ , and the resistivity as  $\rho = \frac{1}{K_0}$ , both beyond the constant-relaxation-time approximation.

*Materials preparation, characterization and measurement*. The powders of  $\text{Na}_{0.71}\text{Co}_{1-y}\text{Fe}_y\text{O}_2$  ( $y = 0, 0.05, 0.10$ , and  $0.15$ ) are prepared by the Pechini method. Stoichiometric amounts of the chemicals: sodium acetate ( $\text{NaC}_2\text{H}_3\text{O}_2$ , 99.0%), Iron (III) nitrate nonahydrate (Sigma-Aldrich, purity 98%), cobalt acetate tetrahydrate ( $(\text{CH}_3\text{COO})_2\text{Co} \cdot 4 \text{H}_2\text{O}$ , 98.0%) and citric acid ( $\text{C}_6\text{H}_8\text{O}_7$ , 99 %, CA) are each dissolved in deionized distilled water. The calculated amount of citric acid and ingredient acetates is mandated at a molar ratio of 1.5:1. The precursor solution is heated in an oil bath at  $65^\circ \text{C}$  while stirring continuously until a uniform viscous gel (2-3 h) forms. Subsequently, ethylene glycol ( $\text{HOCH}_2\text{CH}_2\text{OH}$ , EG,  $\rho = 1.11 \text{ g/cm}^3$ ) is added as a gelling agent in a molar ratio of 3:1 to the amount of citric acid. The gel is dried at  $120^\circ \text{C}$  for 4 hours and then heated in air to  $300^\circ \text{C}$  for 10 hours. The resulting powder is calcinated in air at  $850^\circ \text{C}$  for 20 hours. Densification was done in two steps: cold pressing in air (20kN, 20min) followed by iso-static pressing (800kN, 1min). Finally, the pellets are sintered for 24 hours at  $900^\circ \text{C}$  in air.

The samples' phase structure is identified by the Bruker D8-Advance diffractometer in Debye-Scherrer geometry with (220) Ge monochromator (Mo-K $\alpha$ 1, x-ray

wavelength of  $0.70930\text{\AA}$ ). Seebeck coefficient and resistivity are measured simultaneously with a ZEM-3 (M10) ULVAC system, supplied with Pt electrodes, in the range  $T = 30^\circ - 350^\circ \text{C}$  and 950 mBar oxygen pressure. The uncertainties for both transport properties amount to  $\pm 7\%$ .

XRD patterns are plotted in Fig. 1. For Fe substitution  $> 10\%$  an impurity phase occurs. Thus the experimental study of phase-pure Fe-doped samples is here limited to  $y \leq 0.1$ . Note that an Fe doping of  $\text{Na}_{0.63}\text{CoO}_2$  with  $y \leq 0.03$  has been reported by Zhou *et al.* [39], but without thermoelectric characterization.

*Correlated electronic structure.* The  $\text{Na}_{0.7}\text{CoO}_2$  electronic structure with multi-orbital DMFT self-energy effects has been discussed in Ref. [27]. Electronic correlations are effective in renormalizing the low-energy  $t_{2g}$  band manifold, introducing broadening due to finite lifetime effects and shifting the occupied  $e_g$  pockets further away from the Fermi level (see top of Fig 2a). The single-sheet hole-like FS stems from an  $a_{1g}$  dominated band.

Replacing a fraction  $y$  of cobalt by iron introduces hole doping of the same concentration. The actual transition-metal  $t_{2g}$  filling then reads  $n(t_{2g}) = 5 + x - y \equiv 5 + \tilde{x}$ . We here employ two rather large theoretical Fe dopings of  $y = 0.25, 0.50$  to illustrate the principle effect. Because of the averaged VCA treatment, we underestimate

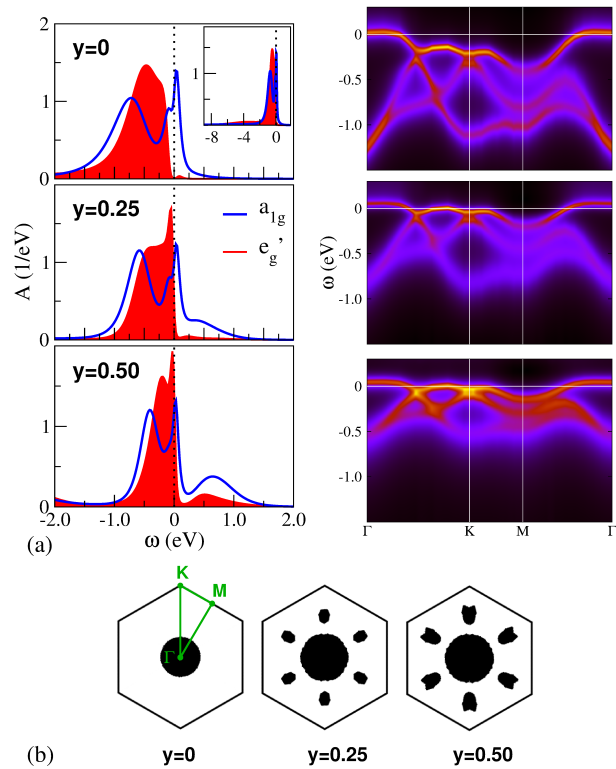


FIG. 2. (color online) DFT+DMFT electronic structure for  $\text{Na}_{0.7}\text{Co}_{1-y}\text{Fe}_y\text{O}_2$ . (a) Spectral function for different  $y$ . Left:  $k$ -integrated  $A = \sum_{\mathbf{k}} A(\mathbf{k}, \omega)$  and right:  $k$ -resolved along high-symmetry lines in the Brillouin zone. (b)  $y$ -dependent FS.

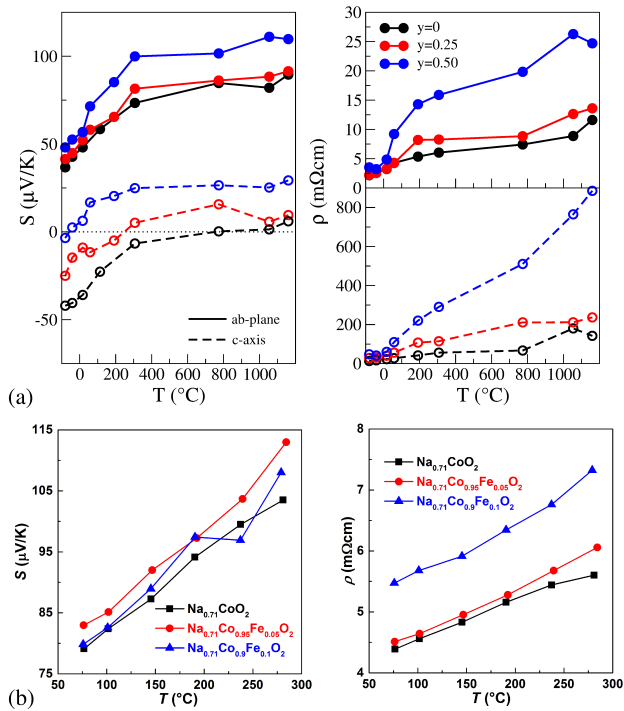


FIG. 3. (color online) Thermopower and resistivity for different Fe doping  $y$ . (a) Theoretical data from DFT+DMFT for  $y = 0, 0.25, 0.50$ . Solid lines: in-plane, dashed lines: along  $c$ -axis. (b) Experimental data for  $y = 0, 0.05, 0.10$ .

its realistic impact and thus the lower experimental dopings yield comparable effective physics. Figure 2 exhibits the changes of the spectral function due to hole doping  $y$ . The  $e'_g$  pockets shift towards  $\varepsilon_F$ , develop a low-energy quasiparticle (QP) resonance and participate already for  $y=0.25$  in the FS. Since the partial bandwidth of the  $e'_g$  derived states is reduced compared to the  $a_{1g}$  one due to smaller hopping, the pocket QP resonance is rather sharp. Additionally the overall renormalization is enhanced with  $y$  and an upper Hubbard band sets in for  $y=0.50$ . This strengthening of electronic correlations is not surprising since the Fe doping effectively drives  $\text{Na}_{0.7}\text{CoO}_2$  again further away from the band-insulating ( $x=1$ ) limit. However importantly, note that systems at a sole Na-doping level  $x_1$  and at effective doping level  $\tilde{x}_1 = x_2 - y \stackrel{!}{=} x_1$  are *not* electronically identical. Lets assume to lower the electron doping starting from  $x=0.7$  where hole pockets are shifted below  $\varepsilon_F$ . Then it was shown in Ref. [27] that for  $x=0.3$  the  $e'_g$  pockets are still suppressed at the Fermi level. But here for  $\tilde{x}=0.7 - 0.25=0.45$  these pockets already cross  $\varepsilon_F$ . Thus Fe doping strengthens the multi-orbital transport character compared to pure-Na doping.

*Theoretical transport.* In Ref. [27] the anisotropic thermopower of sodium cobaltate at  $x = 0.70, 0.75$  has been revealed using the present DFT+DMFT-based multi-orbital Kubo formalism. Here we compare in

Fig. 3a the results with and without Fe doping for  $\text{Na}_{0.7}\text{CoO}_2$ . Quantitatively, the in-plane Seebeck values without Fe doping match the experimental data by Kaurav *et al.* [3]. As a proof of principles, theory documents an enhancement of the in-plane thermoelectric transport compared to the Fe-free case. For once, it may be explained by the increase of transport-relevant electron-hole asymmetry due to the emerging  $e'_g$  pockets at  $\varepsilon_F$ . A Seebeck increase because of this effect was predicted early on by model studies [20], though its realization by Fe doping was not foreseen. In addition, the small negative  $c$ -axis thermopower in Fe-free  $\text{Na}_{0.7}\text{CoO}_2$  eventually changes sign for larger  $y$ . This fosters the coherency of the net thermoelectric transport.

The resistivity also increases with Fe doping and the in-plane values match our experimental data (see below). A gain of scattering because of reinforced electron correlations and appearing interband processes is to be blamed. Though the  $c$ -axis resistivity largely exceeds the in-plane one, the transport anisotropy seems still underestimated compared to measurements by Wang *et al.* [40].

*Experimental transport.* In direct comparison to the theoretical data, Fig. 3b displays the experimentally determined Seebeck coefficient. A clear observation can be extracted, namely Fe-doping gives rise to an increase of the experimental thermopower compared to the Fe-free case. But this enhancement is not of monotonic form with  $y$  and as already remarked, the achievable phase-pure Fe content is experimentally limited to  $y=0.1$ . Still, experiment verifies qualitatively the theoretical prediction on a similar quantitative level in terms of relative thermopower growth. The non-monotonic character might result from intricate real-space effects, e.g. a modification of the Co/Fe local-moment landscape, which are beyond the VCA method that was employed in theory.

The resistivity increase reported in Fig. 3b also verifies the theoretically obtained scattering enhancement. More pronounced correlation effects, the introduced interband scattering for finite  $y$  and/or modified vibrational properties are at the origin of this behavior. Also here, a deeper theoretical analysis beyond VCA, with additional inclusion of the phonon degrees of freedom, is in order to single out the dominate scattering mechanism.

*Conclusions.* Theory and experiment agree in the enhancement of the sodium cobaltate thermopower iron doping. This agreement may serve as a proof of principles for further engineering protocols. Our calculations for Fe-doped  $\text{Na}_{0.7}\text{CoO}_2$  show that effective hole doping takes place. This shifts the originally occupied  $e'_g$ -like pockets to the Fermi level. The increased electron-hole transport asymmetry sustains an enlarged Seebeck coefficient. Iron doping also increases electronic correlations by driving the system further away from the band-insulating regime. Yet the doping is different from a nominal identical hole doping via reducing Na content. This is not of complete surprise since first, the Na atom is here an elec-

tron donor compared to the Fe atom. Second, Na ions are positioned in between the  $\text{CoO}_2$  planes and their contribution to bonding and scattering is rather different from substitutional Fe within the planes.

It would be interesting to further analyze the engineering possibilities of the cobaltate thermopower. Strobel *et al.* [41] already performed experimental studies for doping with Fe-isovalent Ru and also observed a non-monotonic thermopower increase, yet with semiconducting properties. A recent theoretical study of Sb-doped  $\text{Na}_x\text{CoO}_2$  predicted a decrease in thermopower [42]. Generally, correlated materials are much more sensitive to doping than weakly correlated systems because of induced transfer of spectral weight. Another aspect in this regard is the nano-structuring of thermoelectric compounds [43, 44]. Research on such structurings for the case of correlated materials, combined with a tailored chemical doping, in view of increasing the figure of merit is still at its infancy. The novel field of oxide heterostructures could serve as an ideal playground.

We thank L. Boehnke, who coded the Kubo framework in our DFT+DMFT scheme, for very helpful discussions. We are indebted to D. Grieger for further theory discussions, P. Yordanov and H.-U. Habermeier for help with the transport measurements, as well as X. Xiao, J. Moreno Mendaza, and M. Wiedemeyer for assistance in the sample preparation. Financial support from DFG-SPP1386 and WE 2803/2-2 is acknowledged. Computations were performed at the University of Hamburg and the JURECA Cluster of the Jülich Supercomputing Centre (JSC) under project number hhh08.

- 
- [1] I. Terasaki, Y. Sasago, and K. Uchinokura, *Phys. Rev. B* **56**, R12685 (1997).
- [2] T. Motohashi, E. Naujalis, R. Ueda, *et al.*, *Appl. Phys. Lett.* **79**, 1480 (2001).
- [3] N. Kaurav, K. K. Wu, Y. K. Kuo, *et al.*, *Phys. Rev. B* **79**, 075105 (2009).
- [4] M. Lee, L. Viciu, L. Li, *et al.*, *Nat. Mat.* **5**, 537 (2006).
- [5] S. Hébert, W. Kobayashi, H. Muguerra, *et al.*, *Phys. Status Solidi A* **210**, 69 (2013).
- [6] I. R. Mukhamedshin, H. Alloul, G. Collin, *et al.*, *Phys. Rev. Lett.* **94**, 247602 (2005).
- [7] G. Lang, J. Bobroff, H. Alloul, *et al.*, *Phys. Rev. B* **78**, 155116 (2008).
- [8] M. L. Foo, Y. Wang, S. Watauchi, *et al.*, *Phys. Rev. Lett.* **92**, 247001 (2004).
- [9] T. Motohashi, R. Ueda, E. Naujalis, *et al.*, *Phys. Rev. B* **67**, 064406 (2003).
- [10] A. T. Boothroyd, R. Coldea, D. A. Tennant, *et al.*, *Phys. Rev. Lett.* **92**, 197201 (2004).
- [11] H. Sakurai, N. Tsujii, and E. Takayama-Muromachi, *J. Phys. Soc. Jpn.* **73**, 2393 (2004).
- [12] S. P. Bayrakci, I. Mirebeau, P. Bourges, *et al.*, *Phys. Rev. Lett.* **94**, 157205 (2005).
- [13] L. M. Helme, A. T. Boothroyd, R. Coldea, *et al.*, *Phys. Rev. B* **73**, 054405 (2006).
- [14] G. J. Shu, A. Prodi, S. Y. Chu, *et al.*, *Phys. Rev. B* **76**, 184115 (2007).
- [15] T. F. Schulze, M. Brühwiler, P. S. Häflicher, *et al.*, *Phys. Rev. B* **78**, 205101 (2008).
- [16] A. Wilhelm, F. Lechermann, H. Hafermann, *et al.*, *Phys. Rev. B* **91**, 155114 (2015).
- [17] W. Koshibae and S. Maekawa, *Phys. Rev. Lett.* **87**, 236601 (2001).
- [18] H. J. Xiang and D. J. Singh, *Phys. Rev. B* **76**, 195111 (2007).
- [19] N. Hamada, T. Imai, and H. Funashima, **19**, 365221 (2007).
- [20] K. Kuroki and R. Arita, *J. Phys. Soc. Jpn.* **76**, 083707 (2007).
- [21] M. R. Peterson, B. S. Shastry, and J. O. Haerter, *Phys. Rev. B* **76**, 165118 (2007).
- [22] P. Wissgott, A. Toschi, H. Usui, *et al.*, *Phys. Rev. B* **82**, 201106(R) (2010).
- [23] G. Sangiovanni, P. Wissgott, F. Assaad, *et al.*, *Phys. Rev. B* **86**, 035123 (2012).
- [24] M. Z. Hasan, Y.-D. Chuang, D. Qian, *et al.*, *Phys. Rev. Lett.* **92**, 246402 (2004).
- [25] J. Geck, S. V. Borisenko, H. Berger, *et al.*, *Phys. Rev. Lett.* **99**, 046403 (2007).
- [26] G.-T. Wang, X. Dai, and Z. Fang, *Phys. Rev. Lett.* **101**, 066403 (2008).
- [27] L. Boehnke and F. Lechermann, *phys. stat. sol. (a)* **211**, 1267 (2014).
- [28] D. Grieger, C. Piefke, O. E. Peil, *et al.*, *Phys. Rev. B* **86**, 155121 (2012).
- [29] S. G. Louie, K. M. Ho, and M. L. Cohen, *Phys. Rev. B* **19**, 1774 (1979).
- [30] A. N. Rubtsov, V. V. Savkin, and A. I. Lichtenstein, *Phys. Rev. B* **72**, 035122 (2005).
- [31] P. Werner, A. Comanac, L. de' Medici, *et al.*, *Phys. Rev. Lett.* **97**, 076405 (2006).
- [32] L. Boehnke, H. Hafermann, M. Ferrero, *et al.*, *Phys. Rev. B* **84**, 075145 (2011).
- [33] O. Parcollet, M. Ferrero, T. Ayrat, *et al.*, *Comput. Phys. Commun.* **196**, 398 (2015).
- [34] B. Amadon, F. Lechermann, A. Georges, *et al.*, *Phys. Rev. B* **77**, 205112 (2008).
- [35] V. I. Anisimov, D. E. Kondakov, A. V. Kozhevnikov, *et al.*, *Phys. Rev. B* **71**, 125119 (2005).
- [36] V. I. Anisimov, I. V. Solovyev, M. A. Korotin, M. T. Czyżyk, and G. A. Sawatzky, *Phys. Rev. B* **48**, 16929 (1993).
- [37] V. S. Oudovenko, G. Pálsson, K. Haule, *et al.*, *Phys. Rev. B* **73**, 035120 (2006).
- [38] X. Deng, J. Mravlje, R. Žitko, *et al.*, *Phys. Rev. Lett.* **110**, 086401 (2013).
- [39] T. Zhou, D. Zhang, T. W. Button, *et al.*, *Dalton Trans.* **39**, 1089 (2010).
- [40] C. H. Wang, X. H. Chen, J. L. Luo, *et al.*, *Phys. Rev. B* **71**, 224515 (2005).
- [41] P. Strobel, H. Muguerra, S. Hébert, *et al.*, *J. of Solid State Chem.* **182**, 1872 (2009).
- [42] M. H. N. Assadi and H. Katayama-Yoshida, *J. Phys.: Condens. Matter* **27**, 175504 (2015).
- [43] L. D. Hicks and M. S. Dresselhaus, *Phys. Rev. B* **47**, 12727 (1993).
- [44] K. Koumoto, Y. Wang, R. Zhang, *et al.*, *Annu. Rev. Mater. Res.* **40**, 363 (2010).